Progress In Electromagnetics Research Letters, Vol. 35, 1–10, 2012

DOPPLER FEATURES FROM WIND TURBINE SCATTERING IN THE PRESENCE OF GROUND

A. Naqvi*, N. Whitelonis, and H. Ling

Department of Electrical and Computer Engineering, The University of Texas at Austin, Austin, TX 78712-1084, USA

Abstract—We study the Doppler features of electromagnetic scattering from a wind turbine with rotating blades in the presence of ground. Image theory in conjunction with a shooting-and-bouncing ray code, Ahilo, is used to carry out the dynamic signature simulation. The observed features in the simulation are corroborated with laboratory measurements. In addition, the Doppler features from a wind turbine in the presence of a moving ground is simulated and analyzed.

1. INTRODUCTION

The increase in the number of wind farms has created concerns in the radar community due to the radar clutter caused by wind turbines [1, 2]. The large rotating turbine blades can interfere with radar detection of moving targets [1]. In addition, the moving blades may give rise to cross-range artifacts in high-resolution synthetic aperture radar imaging. Understanding the features of the clutter is a first step towards mitigation measures. To this end, previous studies have documented in detail the time-varying Doppler characteristics of wind turbines [3, 4]. Recently, concerns regarding the effects of ground on turbine scattering and how to account for these effects were raised in [5, 6]. Ground interactions could play an important role in scenarios where the radar is elevated high above the ground, such as those found in airborne surveillance systems. However, the mechanisms behind the presented results in [5, 6] were not described or explained. The physics of ground scattering for targets situated above ground is generally considered well understood in the electromagnetics community, and has been previously applied to simulate Doppler tracks of a moving human above ground [7].

Received 10 August 2012, Accepted 5 September 2012, Scheduled 13 September 2012
* Corresponding author: Aale Naqvi (aalenaqvi@yahoo.com).

In this paper, we report on and provide a detailed analysis of the Doppler features that arise in wind turbine scattering due to ground bounces. First, we present Doppler features from turbine blades rotating above a stationary ground. Simulations are carried out using the high-frequency shooting-and-bouncing-ray code Ahilo [8]. The method of images is employed to account for the infinite ground plane. This allows for a rigorous accounting of ground effects without the need to model a large ground plane in the electromagnetic simulation. Doppler spectrograms are obtained using the short-time Fourier transform (STFT) and the tracks that arise from ground effects are identified and interpreted. In addition to the simulations, measurements are carried out on a rotating rod in the vicinity of a large metal ground plane to corroborate the simulation results. Finally, we report on Doppler features that arise in the case of a rotating turbine above a moving ground based on Ahilo simulation.

2. DOPPLER FEATURE ANALYSIS

The presence of ground introduces complexity to the returned signal due to the target-ground interactions in addition to the direct return from the target. Simulations are performed to investigate the time-varying Doppler features that arise from target-ground interactions. Figure 1(a) shows the CAD model of the turbine used in this paper. It contains the major components in a commercial turbine, including three blades, the nacelle and the tower. The size of the tower is 64 m, the radius of the hub is 2 m, and the length of each blade is 35 m. Figure 1(b) depicts the interaction of a turbine with the ground. The solid and dashed arrows in Figure 1(b) indicate the incident and scattered waves, respectively. With ground interactions, new Doppler tracks in addition to the strong blade flashes and weak tip halos previously documented in [3, 4] are expected in the time-dependent Doppler spectrum.

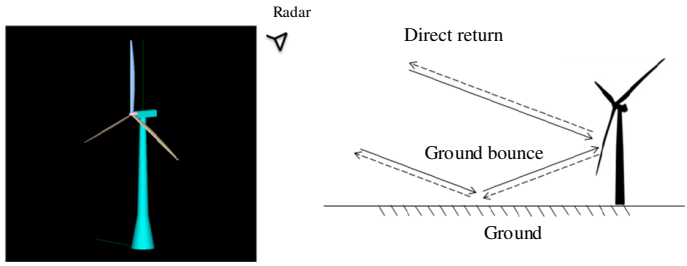

Figure 1. (a) Turbine CAD model. (b) Ground interactions.

For simulation, the radar frequency is set to 1 GHz and the radar is located at an elevation angle of 20° with respect to the ground. The polarization is horizontal. The turbine is assumed to be at a 90° yaw angle with respect to the radar (i.e., edge-on incidence). To perform the dynamic simulation, the backscattered data are collected for each snapshot of the blade orientation, in 0.1° increments, over one complete revolution of the turbine blades. The built-in 'rotation' feature of Ahilo for a pre-defined portion of the target provides a convenient means to collect backscattering from the turbine. To simulate far-field backscattering from the turbine rotating above the ground, image theory is used [9]. The image of the real turbine is created and placed so that it forms a mirror image of the real turbine in the CAD model. This is done for each snapshot of the blade orientation. Consequently, the blades of the real turbine and those of its image rotate in opposite directions. To generate the total scattered field, first, monostatic data are collected with the source and observer located at the radar position. Second, bistatic data are collected with the incident wave originating from the image source position and the observer located at the real radar position. The superposition of the two simulated data sets gives the total scattered signal from the turbine in the presence of ground. The data are then processed using the STFT with a time window of 0.3 second for an assumed rotation rate of 12 rpm. Figures 2(a) and 2(b) show respectively the spectrogram for a turbine rotating in free space and a turbine rotating in the presence of ground. For the turbine in free space, the key Doppler features come from blade flashes, labeled (i) in Figure 2(a), that occur every 60° rotation of the turbine blades. Every positive Doppler flash is followed by a negative flash. Weak tip halos can also be observed that are due to scattering from the blade tips. In Figure 2(b), two additional flashes accompanied by tip halos are present. These additional features are due to the presence

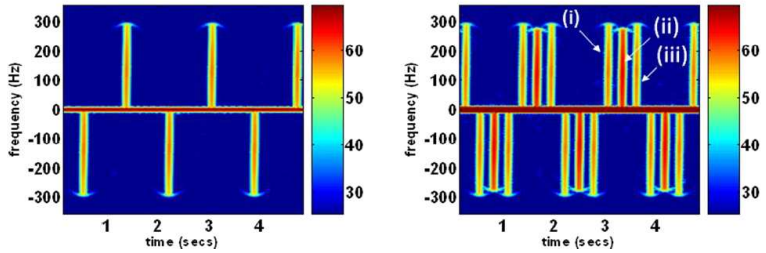

Figure 2. Spectrogram from turbine backscattering. (a) Without ground. (b) In the presence of ground.

of the ground. Figures 3(a), 3(b) and 3(c) illustrate respectively the mechanisms giving rise to flashes labeled (i), (ii) and (iii) in Figure 2(b). Figure 3(a) is the direct flash mechanism between the radar and the blade that gives rise to flash (i). Figure 3(b) shows the bistatic specular reflection mechanisms between the image source and the blade (or its image). These two mechanisms correspond to the two single-ground-bounce mechanisms and give rise to the flash labeled (ii) in Figure 2(b). It occurs in time after the direct flash for the assumed counter-clockwise rotation of the blades. The time interval between these flashes is a function of the elevation angle and the rotation speed of the turbine. Figure 3(c) shows the specular reflection mechanism between the radar and the image blade that correspond to the double-ground-bounce flash labeled (iii) in Figure 2(b). It occurs yet later in time. Note that the maximum Doppler of (ii) is less than that of mechanisms (i) and (iii) because the radial velocity of the blade relative to the source and observer is less than those in the other two cases. On the other hand, the strength of feature (ii) is 3 dB higher than flashes (i) and (iii) since there are two single-ground-bounce mechanisms that are reciprocals of each other. They have identical Doppler returns. The single-ground-bounce mechanism also produces a specular reflection from the tower which is the reason for the much stronger DC-frequency component in Figure 2(b) relative to Figure 2(a). Aside from the single- and double-ground-bounce interactions described, no other Doppler flashes or higher-order features with strong intensities are observed. For example, no noticeable blade-ground-blade interaction is seen. This is due to a combination of the weaker scattering from two bounces off the blades and the shadowing from other blades. While the simulation results presented here are for an elevation angle of 20°, increasing the elevation angle will simply lead to an increase in the time lags between the three flashes and a decrease in the maximum Doppler of the single-ground-bounce flash. Also, although only results for the horizontal polarization are shown here, we did not find a strong polarization dependence due to the large electrical size of the structure. The vertically polarized simulation gave essentially identical Doppler features as the horizontally polarized case. Finally, while we have analyzed the highly idealized geometry of a perfect conducting, infinite ground plane, an effective reflection coefficient approach can be used to model non-perfect-conducting, rough or even non-flat terrains [10, 11]. However, that will only change the intensity of the ground-bounce features.

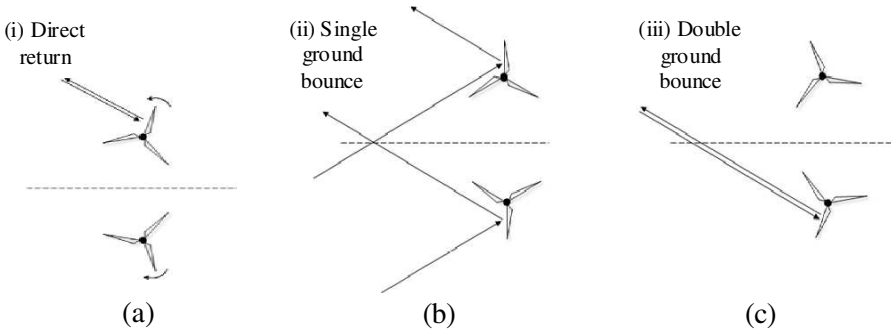

Figure 3. Image theory applied to simulate and explain the observed flashes. (a) Direct return flash. (b) Single-ground-bounce flash. (c) Double-ground-bounce flash.

3. EXPERIMENTAL CORROBORATION

Having simulated and analyzed the turbine Doppler features in the presence of ground, we next corroborate the simulations with laboratory measurements. A rotating metal rod of length 0.6 m and radius 1.2 mm is rotated about one end on a turn-table with a large conducting ground plane placed next to the rod. The minimum distance between the rod's end-tip and the ground plane is 0.5 m. Figures 4(a) and 4(b) are respectively the schematics and a photo of the measurement setup. Figures 4(c) and 4(d) show the corresponding measured results. Backscattering measurements are carried out using a vector network analyzer (*Agilent N5230A*) in continuous wave (CW) mode at 14 GHz. The choice of this frequency is a compromise, as our instrumentation cannot reach the frequency needed (1 GHz $*$ (35 m/0.6 m) $=$ 58 GHz) to produce a faithful scaled model measurement of the turbine size studied in the simulation. Data are collected for 420 seconds, which correspond to one rotational period of our turn-table, while the sampling rate is set at 3.4 Hz. This corresponds to backscattering being collected every 0.25° of rotation. The slow sampling rate, 3.4 Hz, allows for a low intermediate frequency (IF) bandwidth setting to minimize the background noise in the data. A horn antenna, separated by 1.6 m from the center of rotation for the rod is used to collect S_{11} measurements. The complex scattering data are first processed using a near-field-to-far-field transform algorithm [12] to correct the near-field effect due to the close position of the horn to the target. Subsequently, the data are processed using the STFT with a 30-second time window. Figures 4(c) and 4(d) respectively show the resulting spectrogram from

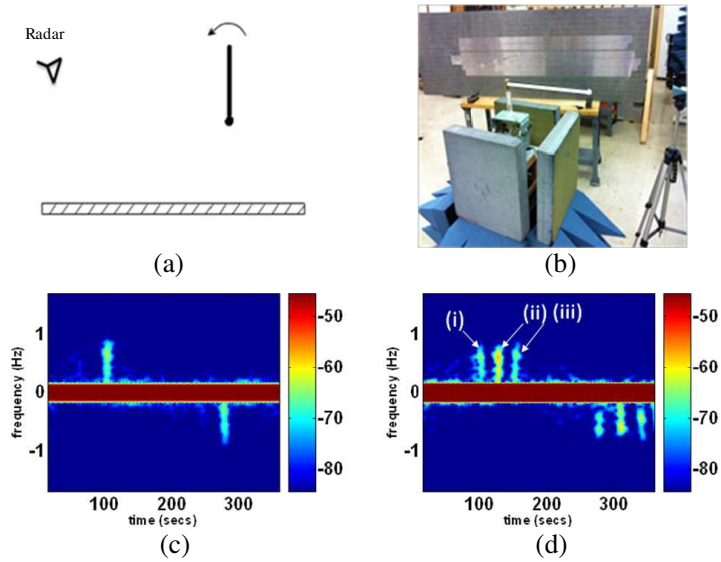

Figure 4. Measurement setup. (a) Schematics. (b) Photo. Spectrogram from measurement data. (c) Without ground. (d) In the presence of ground.

the measured data for the rotating rod in free space and in the presence of ground. The very strong DC lines in both figures are due to the self-reflection from the mouth of the horn. Figure 4(c) shows the direct flashes from the blades whereas Figure 4(d) shows two additional blade flashes. It is observed that the measured blade flashes corroborate the simulated blade flashes in Figures 3(b) and 3(c) very well. The labels (i), (ii), and (iii) are respectively the direct, single-ground-bounce, and double-ground-bounce interactions illustrated in Figure 3. Similar to the simulations, the single-ground-bounce feature is stronger in strength than the direct and double-ground-bounce returns.

4. GROUND MOTION

Having analyzed turbine interactions with a stationary ground, we move on to study the case of a moving ground, which may have implications in the Doppler features of offshore turbines situated on a moving sea surface. We assume the entire ground moves sinusoidally in the vertical direction and again apply image theory to simulate this scenario. For this case the turbine and its image can be considered to be a single tower with twice the length and having rotating blades on each end. Upon motion of the ground, the motion of the "image end"

of the tower moves up and down, while the "real end" of the tower remains stationary. This motion is similar to how a mass on a spring moves. With motion of the ground, the image source will also have an up-and-down motion imparted to it. A displacement of ground by an amount d corresponds to a displacement of $2d$ in the image source and the image end. Realizing this dynamic scenario exactly in the Ahilo simulation requires detailed editing of the CAD file for each time snapshot. This is quite laborious, and we instead use an approximate scheme to carry out the simulation.

We assume the major scattering contributions come from: (1) the direct monostatic return from the real turbine shown in Figure 3(a), (2) the single-ground-bounce return from the real turbine and its image, which is the bistatic return depicted in Figure 3(b), and (3) the double-ground-bounce return from the image turbine shown in Figure 3(c). The time-varying returns from the three contributions are computed separately and then summed. In computing the return from each contribution, we neglect the slight change in the tower height as a function of time. The direct return (1) is not affected by the ground motion and is computed first. The bistatic return (2) is computed as follows. Backscattering is collected in the same manner as the stationary ground case with rotating blades. The ground motion is then injected into the signal by adding an extra phase at each snapshot of the turbine position during the course of its rotation. Given the received signal in the case of static ground, E^{stat}, the motion of the ground is incorporated as

$$E(t) = E^{stat}(t) \exp\left[-j\left(\vec{k}^{i} - \vec{k}^{OB}\right) \cdot \vec{r}'(t)\right] \tag{1}$$

where $\vec{k}^{i}$ is the incident wave vector, $\vec{k}^{OB}$ is the observation wave vector, and $\vec{r}'(t)$ is the time-dependent position vector describing the displacement of the image turbine relative to the hub of the real turbine. The dot product ensures that the radar only registers the radial component of the ground displacement. The double-ground-bounce return (3) is computed from the image turbine in a similar fashion as that for return (2), i.e., the phase shift is added using Eq. (1). By simulating returns (1) and (3) separately, we assume no interaction between the real turbine and its image takes place. This is a good approximation since no interactions between the two are observed for the stationary ground case, when the exact image theory is used.

Figure 5(a) shows the spectrogram of the backscattered signal generated by the above methodology. In this case, the maximum ground displacement is set to 7 m and the period of the vibration is 9 seconds. The wavelength of the water waves in shallow water is

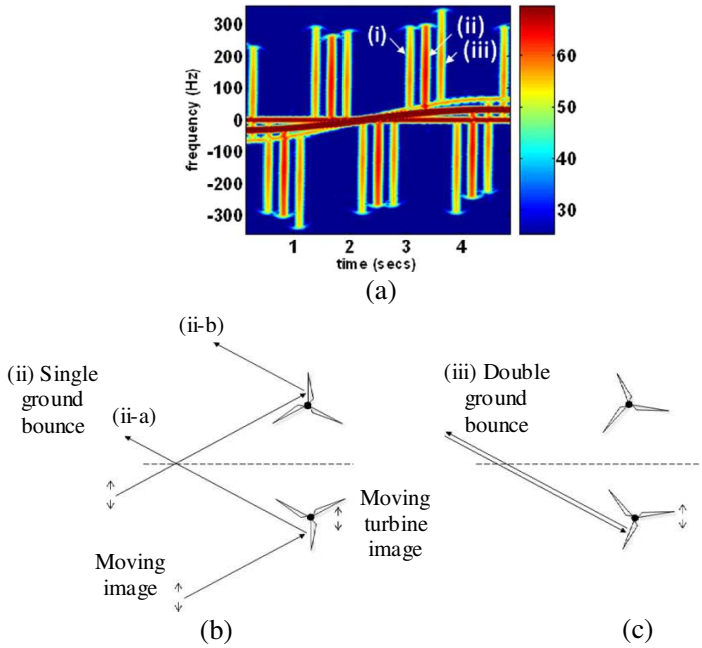

Figure 5. Backscattering from a turbine in the presence of a sinusoidally vibrating ground. (a) Spectrogram from backscattered data. (b) Single-ground-bounce return corresponding to track (ii) in (a). (c) Double-ground-bounce return corresponding to track (iii) in (a).

on the order of 100 m or more. On the other hand, the estimated Fresnel zone spot size on the water surface at 1 GHz for the chosen parameters is on the order of tens of meters. Therefore, the locally flat ground approximation would be an adequate assumption in this case. In comparison to Figure 2(b), it is observed that the direct blade flash labeled (i) is not affected, while the two ground-bounce-induced blade flashes ride on sinusoidal tracks that result from the ground plane motion. Figures 5(b) and 5(c) demonstrate the mechanisms responsible for the observed bobbing of the flashes. Figure 5(b) shows the single-ground-bounce mechanism that gives rise to the bobbing motion of its corresponding flash labeled (ii) in Figure 5(a). Figure 5(b) demonstrates the path of the wave from the image source to the turbine blades and back to the observation point. In the interaction labeled (ii-a), the wave encounters a path length change as it travels back towards the observer. For interaction labeled (ii-b), the wave encounters a change in path length when the incident wave hits the real turbine

blades. Both interactions give rise to identical Doppler, therefore, their corresponding flashes remain in phase. Figure 5(c) shows the double-ground-bounce mechanism responsible for the bobbing motion of the flash labeled (iii) in Figure 5(a). Thus, with ground motion, the single- and double-ground-bounce interactions ride on the motion of the ground plane. In addition, the return from the tower also acquires a non-DC return due to the ground motion.

5. CONCLUSION

The Doppler characteristics of electromagnetic backscattering from a wind turbine in the presence of ground have been simulated and studied. We employed a ray-tracing simulation and image theory to acquire backscattered data. It was shown that the presence of ground gives rise to two additional blade flashes between the radar and the turbine. No other flashes or higher-order features with strong intensities were found. The observed features were corroborated with measurements of a simplified wire model. The effects of a moving ground were also simulated and interpreted in detail. Although the geometries analyzed in this paper are for a perfectly conducting, flat ground plane, an effective reflection coefficient approach can be used to model non-perfect-conducting, rough or even non-flat terrains. Appropriate reflection coefficients can be applied to modify the strength of the return signal based on the size of the Fresnel zone projection on the ground relative to the scale-length of the ground roughness. However, that is not expected to change the Doppler features reported in this paper.

ACKNOWLEDGMENT

This work was supported by the Department of Energy under Grant DE-EE0005380, by the National Science Foundation under Grant ECCS-1232152, and in part by the Texas Norman Hackerman Advanced Research Program under Grant No. 003658-0065-2009. The authors are grateful to Dr. Andy Lee for providing the use of Ahilo for this work and Dr. Rajan Bhalla for providing the turbine CAD model.

REFERENCES

1. Report to the Congressional Defense Committees on The Effect of Windmill Farms On Military Readiness, Office of the Director of Defense Research and Engineering, Undersecretary for Space and Sensor Systems, Aug. 2006.

2. Sandifer, J. B., T. Crum, E. Ciardi, and R. Guenther, "A way forward: Wind farm — Weather radar coexistence," *Proc. Windpower 2009*, Chicago, IL, May 2009.
3. Kent, B. M., A. Buterbaugh, K. C. Hill, G. Zelinski, R. Hawley, L. Cravens, T. Van, C. Vogel, and T. Coveyou, "Dynamic radar cross section and radar Doppler measurements of commercial general electric windmill power turbines part 1 — Predicted and measured radar signatures," *IEEE Antennas Propag. Mag.*, Vol. 50, 211–219, Apr. 2008.
4. Naqvi, A., S. Yang, and H. Ling, "Investigation of Doppler features from wind turbine scattering," *IEEE Antennas Wireless Propagat. Lett.*, Vol. 9, 485–488, 2010.
5. Greving, G., W. Biermann, and R. Mundt, "Wind turbines as distorting scattering objects for radar-clutter aspects and visibility," *Proc. Int. Radar Symp. 2010*, Vilnius, Lithuania, Jun. 2010.
6. Greving, G., W. Biermann, and R. Mundt, "On the relevance of the measured or calculated RCS for objects on the ground — Case wind turbines," *Proc. 3rd European Conf. Antennas Propagat.*, 2216–2220, Berlin, DE, 2009.
7. Ram, S. S., R. Bhalla, and H. Ling, "Simulation of human radar signatures in presence of ground," *IEEE Antennas Propagat. Soc. Int.. Symp. Dig.*, Charleston, Jun. 2009.
8. *AHILO: Computer Code for Solving Electromagnetic Problems*, Jan. 12, 2012, http://www.ahilo.net/AHILO_web/Overview.html.
9. Balanis, C. A., *Advanced Engineering Electromagnetics*, 314–325, New Jersey, Wiley, 1989.
10. Wang, X., C.-F. Wang, Y.-B. Gan, and L.-W. Li, "Electromagnetic scattering from circular target above or below rough surface," *Progress In Electromagnetics Research*, Vol. 40, 207–227, 2003.
11. Vaitilingom, L. and A. Khenchaf, "Radar cross sections of sea and ground clutter estimated by two scale model and small slope approximation in HF-VHF bands," *Progress In Electromagnetics Research B*, Vol. 29, 311–338, 2011.
12. Whitelonis, N., S. Yang, and H. Ling, "Application of near-field to far-field transformation to Doppler features from wind turbine scattering," *IEEE Trans. Antennas Propagat.*, Vol. 60, 1660–1665, Mar. 2012.